Structurally Colored Thin Films of Ca^{2+}-Cross-Linked Alginate

Matthew D. Cathell and Caroline L. Schauer*

Department of Materials Science and Engineering, Drexel University, Philadelphia, Pennsylvania 19104

Received May 4, 2006; Revised Manuscript Received August 11, 2006

Alginate, or alginic acid, is an unbranched binary copolymer of (1→4)-linked β-D-mannuronic acid and α-L-guluronic acid. Alginate readily forms binding interactions with a variety of divalent metal ions, such as calcium. This binding has been used to cross-link bulk alginates for a wide variety of applications, particularly in areas of tissue engineering, medical devices, and wound-healing dressings. A new method is identified here for producing Ca^{2+}-cross-linked thin films of sodium alginate, using an aerosolized spray of $CaCl_2$ solution. These thin films exhibit structural color that varies with film thickness. It is demonstrated that this structural color is highly reproducible and can also be tuned to produce a wide range of colored films. The noted ability of alginates to bind metal ions is used in combination with the structural coloration afforded by the thin film structure as a basis for color-based optical sensing of metal ions in aqueous solutions. Changes in film thickness, refractive index, and reflectivity in response to metal ions have been measured and reported. For certain ions such as Cr(III) and Cr(VI), changes in film thickness are the predominate factors in shifting the reflected film color. In the case of other ions such as Pb(II), a change in film refractive index plays a significant role in the reflectance properties of films.

Introduction

Structurally Colored Thin Films. Materials that modulate light, such as irises, lenses, and reflectors, are among the most intricate structures found in nature. Many organisms achieve reflectivity by modulating incident sunlight or bioluminescence through a process known as structural coloration.[1−4] Structural color is caused by the interaction of light with nanoscale periodic structures. When light encounters materials with minute structural features (on a size scale comparable to that of light wavelengths themselves), it is subject to a variety of optical effects including single- and multiple-layer thin film interference, diffraction grating effects, photonic crystal effects, liquid crystal effects, and scattering.[5−7]

A number of nature's most colorful creatures, including many insects and marine animals, reflect vibrant colors using a mechanism of stacked, thin layers of biomaterials.[4] These stacked structures act as one-dimensional photonic crystals, allowing selective reflection of certain wavelengths of light, while negating other wavelengths by out-of-phase interference. A single- or multiple-layer biopolymer thin film of appropriate thickness is capable of mimicking this type of natural system. These thin films reflect structural colors that are independent of any intrinsic color, derived from electronic-based light absorption, which the polymer might possess. The colors of structurally colored films shift according to Bragg's law, in which the optical path length is a function of the film thickness and index of refraction. Light reflecting from the air−film surface undergoes constructive and deconstructive interference with light reflected at the underlying polymer−substrate interface, leading to selective wavelength reflection.

Structurally colored thin films have a variety of potential applications, including use as novel reflective and camouflage materials and as a platform for optics-based sensing. This latter point of interest has been the subject of several prior investigations.[8,9] It has been demonstrated that thin films of structurally colored polymers can undergo perceptible color shifts when exposed to selected analytes, such as metallic ions. Past work has focused on thin films of poly(allylamine) and the biopolymer chitosan (a soluble form of chitin), which were found to have optical response to certain cations in aqueous solution.[8,9]

The changes in color observed as a response to dissolved analytes may be attributed to a combination of two factors. First, the polymer−analyte interaction may lead to a change in the optical properties of the film by altering its index of refraction. For instance, cation exchange or the sorption of metallic ions can change the effective refractive index of a film, leading to a shift in its reflected color. Alternatively, the analyte species may cause three-dimensional conformational changes in the film, physically altering the optical path length distance. This conformation effect may occur when analytes bind or otherwise interact with polymer chains, or when analytes change the film's equilibrium water content and cause shrinking or swelling.

Alginate Thin Films. Alginates are a family of unbranched binary copolymers of (1→4)-linked β-D-mannuronic acid (M) and α-L-guluronic acid (G) groups (Figure 1a). Alginates with various M and G compositions are produced by a number of organisms and are constituents in the cell walls of brown algae.[10−12]

Alginates interact with a variety of metallic species through several mechanisms, including electrostatic and ionic interactions, covalent-like bonding, coordination, and redox reactions.[12−16] This ability to bind and adsorb metals has led to alginate's use for recovery of both toxic pollutants and precious metals from aqueous effluents.[12,17−19] By making use of alginate's ability to bind metals, the potential sensing capabilities of alginate thin films were investigated. If the binding of ions causes physical changes in thickness or optical changes in refractive index, the reflectance color profile of a film is correspondingly altered. In cases where the reflectance shift is sufficiently pronounced, it becomes possible to visually detect a change in color with the unaided eye.

* To whom correspondence should be addressed. E-mail: cschauer@cbis.ece.drexel.edu.

10.1021/bm060433f CCC: $37.00
Published on Web 11/30/2006

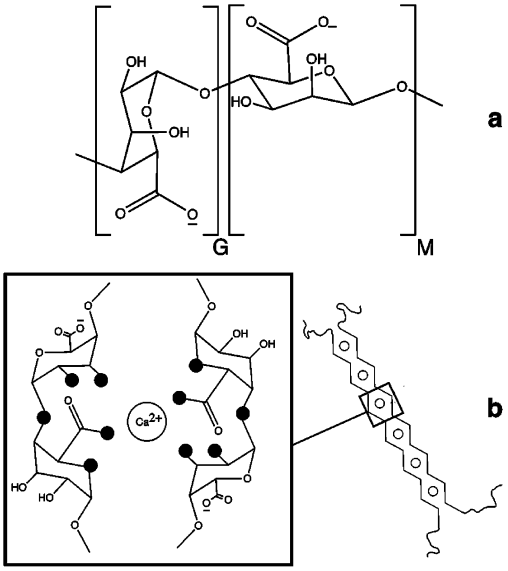

Figure 1. (a) Alginate is a biopolymer made up of randomly assembled subunits of guluronic acid (G) and mannuronic acid (M). Alginates exist with a variety of ratios and sequencing of these G and M blocks, imparting a range of different polymer properties. (b) Alginate cross-linking readily occurs in the presence of divalent calcium ions. Regions of the alginate chain rich in G subunits, which order into "zigzag" structures with cavities of appropriate size for divalent metals, have heightened specificity for Ca^{2+} because of favorable geometric ordering for coordination. A number of oxygen atoms (shown as darkened circles) participate in this coordination arrangement. This system is commonly referred to as the "egg-box" model.

To measure the response of alginate films to aqueous metal salts, it is necessary to first make the polymer water-stable through cross-linking. Cross-linking of the alginate thin films was achieved through binding of divalent calcium ions, a well-known strategy used for cross-linking bulk alginate materials. A great deal of research has been published on alginate's propensity for heightened viscosity and gelation in response to multivalent cations.[20−24] Bulk calcium-cross-linked alginate has been used in numerous applications, particularly in areas of tissue engineering, medical devices, wound-healing dressings, and drug delivery systems.[25−28] Because Ca^{2+} (in concentrations high enough to ensure thin film stability) causes gelation of alginate almost instantly, we were unable to use typical Ca^{2+}-cross-linking procedures for our alginate films. A new method is identified here for producing heavily cross-linked alginate thin films, using a procedure that allows for controlled exposure of the polymer to an aerosolized spray of dissolved $CaCl_2$ in aqueous solution. These films possess excellent water stability and are resistant to water-induced thickness changes. In contrast, studies of structurally colored thin films of covalently cross-linked chitosan have indicated a notable drop in film thickness with water exposure.[8]

The negatively charged carboxylate groups make up the largest component of titratable sites along the alginate backbone and are key to alginate's cross-linking and metal-binding mechanisms. It has been noted that many metals exhibit maximum sorption behavior at pHs correlating to the dissociation constant of carboxylic acids in brown algal materials.[12] Literature values for the pK_a of alginate have been reported in the range of 3.38−3.65, depending on the relative concentrations of mannuronic and guluronic acid subunits.[29] For an intermediate structure containing both residues and a pK_a of 3.44, it is reported that the carboxyl groups along the alginate backbone are deprotonated above pH 6.0,[11] thereby making the groups available to stabilize cation binding. However, there is significant evidence that charge interactions between carboxyl groups and metal ions do not, by themselves, adequately describe the binding observed in cation-induced gelation.

Studies published in 1961 by Schweiger indicated that acetylation of alginate hydroxyl groups inhibited gelation in the presence of divalent ions, suggesting that carboxyl groups are not solely involved in the binding process.[23,30] Rees and Grant et al. proposed the binding of divalent cations occurs in the context of a coordination sphere, involving oxygen atoms from carboxyl and hydroxyl groups, as well as from the ring and glycosidic linkage (Figure 1b).[31,32] Variations in the exact steric arrangement of the coordination sphere have been proposed from X-ray diffraction and NMR spectroscopy studies,[33,34] but the basic coordination principle is well-accepted. A key feature of this complexation theory is that ring oxygen and axial O-1 of guluronic acid subunits form a favorable coordination geometry for multidentate binding of divalent cations, compared with the less favorable geometry achieved by mannuronic acid's equatorial O-1 atom. Blocks of repeated guluronic subunits present rich metal-binding opportunities and can be represented by the "egg-box" model illustrated in Figure 1b, in which a series of divalent calcium (or other cations) are coordinated within the G-block segments of the alginate chain, similar to the packing of eggs in a carton.

It is pertinent to note that the alginate salt used in our study consists of 69% M and 31% G subunits, as reported by the supplier. It should be expected that alginates with other M/G ratios would exhibit differences in metal ion selectivity and/or sensitivity. This phenomenon has been observed and commented upon in a variety of publications in recent decades.[17,22,29,31,35]

Experimental Section

Materials. Alginic acid sodium salt from brown algae, ethylenediaminetetraacetic acid (EDTA), and all metallic salts were purchased from Sigma-Aldrich. The alginate salt had an approximate mannuronic/guluronic ratio of 1.56, a degree of polymerization range of 400−600, and a molecular weight range of 80000−120000. Metallic salts used include chromium(VI) oxide, mercury(II) nitrate monohydrate, lead(II) nitrate, cadmium(II) chloride, arsenic(III) oxide, sodium nitrate, cobalt(II) acetate, disodium hydrogen phosphate, sodium chloride, sodium sulfate, lead(II) acetate, nickel(II) sulfate heptahydrate, sodium acetate, chromium(III) nitrate nonahydrate, and chromium(III) chloride. Calcium chloride solution (2.75%) was obtained from VWR. All chemicals were used as received. Room-temperature ultrapure water (Millipore QPAK system) was used to make all solutions and for silicon wafer cleaning and film rinsing procedures.

Thin Film Deposition and Cross-Linking. Quantities of sodium alginate, ranging from 0.2 to 0.4 g, were dissolved in 30 mL aliquots of ultrapure water. The solutions were filtered in bulk through a coarse fritted glass filter funnel and degassed in a sonicator for 5 min. Further filtration was performed using 0.8 μm Nalgene syringe prefilters (VWR). Small amounts of solutions (~0.3 mL) were dispensed onto fragments of polished silicon wafers (of typical area 6.25 cm^2). The silicon wafers had been previously cleaned using a modified RCA protocol.[8] Thin films were produced by spin coating the wafers in a WS-400B-GNPP/LITE/AS spin processor (Laurell Technologies, North Wales, PA) operating at speeds between 1000 and 4000 rpm for 30−60 s. After coating, the films were dried under a stream of argon while on a hot plate at the lowest temperature setting.

To achieve cross-linking, an aerosol spray of 2.75% calcium chloride solution was applied to the films for periods ranging from 10 s to several minutes. The films were then rinsed for 10 s in ultrapure water and dried again under an argon stream on a hot plate.

EDTA Treatment. To establish Ca^{2+} ions as the thin films' cross-linking agent, cross-linked samples were exposed to EDTA, a calcium chelator. Solutions of EDTA at concentrations of 0.001, 0.01, and 0.1 M were made using ultrapure water and neutralized with 5 M NaOH. Cross-linked alginate films on small fragments of silicon wafer were placed in shallow sample dishes with 20 mL of the EDTA solutions. Film samples immersed in ultrapure water for the same period of time served as a control. After 5 min, the liquids were decanted from the sample dishes and the samples were dried. Thickness, refractive index, and reflectance measurements were made before and after EDTA treatment for comparison.

FTIR. FTIR studies on alginate samples were carried out using an Excalibur FTS-3000 FTIR instrument (Digilab). Spectra were obtained in transmission mode from samples in KBr pellets. A drop of sodium alginate solution was placed between two glass microscope slides to form a flat liquid film. The liquid was allowed to evaporate, producing samples several times thicker than the thin films prepared on the spin-coating apparatus. However, the surface area to volume ratio was deemed acceptable for this investigation of thin film cross-linking.

One of the film samples was sprayed with an aerosol of $CaCl_2$ solution. After 10 s of exposure, the sample was rinsed under ultrapure water and dried under argon. The second sample was examined without $CaCl_2$ treatment. The films were carefully peeled from the slide surfaces and incorporated into KBr pellets for FTIR analysis.

Ion Studies. To test the response of alginate thin films to dissolved metal species, aqueous solutions were made containing 50 ppm concentrations of several metallic cations and pertinent counteranions. Alginate films were placed in sample dishes containing 20 mL of the solutions. After 5 min, the liquids were decanted and the films dried under argon on a warm hot plate. Ellipsometry and reflectance data were gathered for each sample and compared with data obtained prior to ion exposure. Film thicknesses and indices of refraction were determined using an M-2000U variable-angle spectroscopic ellipsometer (J.A. Woollam Co., Lincoln, NE).

An ellipsometer measures changes in the phase and polarized state of an electric field upon reflection to calculate information about a sample's physical and optical properties—in this case, the thickness and refractive index of a biopolymer thin film.[37−39] The data provided by the instrument are the Stokes parameters Ψ and Δ, which are related to the Fresnel reflection coefficients of light parallel and perpendicular to the plane of incidence, R_p and R_s.[40] The ratio of the Fresnel coefficients, called the reflection coefficient ratio, is given by the expression

$$R_p/R_s = \tan(\Psi)\, e^{i\Delta} \quad (1)$$

Data from the alginate thin films were gathered over a wavelength range of 200−1000 nm at a typical reflectance angle of 60°.

The refractive indices of the films were calculated using the Cauchy parametrization function, which yields the refractive index dispersion as a function of the wavelength, λ (μm). The thin films were analyzed using the first three Cauchy fit parameters, *A*, *B*, and *C*:

$$n(\lambda) = A + \frac{B}{\lambda^2} + \frac{C}{\lambda^4} \quad (2)$$

All refractive index values presented in this study are reported at a wavelength of 589.3 nm (the mean sodium D-line). Fitting was performed with the WVASE32 software (J.A. Woollam Co.) using a Levenberg−Marquardt regression algorithm to minimize the mean standard error (MSE) between the experimentally obtained Ψ and Δ terms and model curves. This fitting was accomplished through adjustment of the Cauchy parameters and thickness in a series of error minimization calculations. Convergence was reached when the algorithm was unable to minimize the MSE through further iterations, yielding the reported thickness and refractive index measurements.

Using thickness and refractive index dispersion data gathered from the ellipsometer, model reflectance data were generated in WVASE32 to predict wavelength reflection. The modeling parameters chosen included an unpolarized broad-band light source back-reflected at an angle normal to the film surface, with the assumption that the optically dense silicon substrate would require no backside correction. The generated model reflectance profiles were compared with experimental reflectance data measured with the reflectance spectrometer. The reflectance spectrometer used was a USB2000 miniature fiber optic spectrometer with DH-2000 deuterium tungsten halogen light sources (Ocean Optics, Dunedin, FL). Experimental reflectance data were measured normal to film surfaces.

Each measurement was performed with three replicate samples, with the error reported as the standard error of the mean (SEM) between replicates. Statistical calculations using paired *t* tests were performed to determine whether statistically significant changes in thicknesses, refractive indices, or reflection maxima occurred after immersion of the films in the 50 ppm ion solutions.

Profilometer Study. The physical and optical properties of thin films are strongly coupled, and it can be challenging to discern which component has shifted to alter a film's reflectance properties. To confirm our measurements of the relative contributions of thickness and refractive index effects to the color shift, an optical white light profilometer (Zygo Corp., Middlefield, CT) was used to corroborate thickness changes of two groups of alginate films, consisting of three replicate samples per group.

An artificial step was scratched in each film using a razor blade, and the height difference between the film surface and the underlying substrate was measured along 10 nearby points in the region of the scratch. Each film was then placed in a metal ion solution for 5 min. One group of films was immersed in an ion solution believed to cause predominantly physical changes in the film thicknesses. The second group was exposed to an ion solution in which both significant physical and optical changes were indicated. After solution exposure, the films were dried under argon on a hot plate and measured again on the profilometer to determine the thickness change. These results were compared with those determined using the ellipsometer.

Results and Discussion

Initial attempts to create a calcium alginate film consisted of several different cross-linking techniques. First, various amounts of $CaCl_2$ solution were added to alginate solutions prior to spin coating. Because of the rapidity of cross-linking, insoluble alginate gels formed before films could be produced. The difficulty of producing homogeneous gels through direct mixing has been previously noted, as the alginate and calcium are likely to form a dispersion of gel lumps.[16] Other attempts were made to incorporate Ca^{2+} into the films during spin coating with the use of an automated dispensing mechanism attached to the spin processor. This device controllably released a stream of $CaCl_2$ solution over the silicon wafer as it was being coated. However, cross-linking occurred only in small, localized regions where the $CaCl_2$ solution initially contacted the film surfaces, leaving portions of the film un-cross-linked and, thus, soluble. Cross-linking by direct immersion of films into $CaCl_2$ proved successful in some cases, although this technique sometimes led to a disruption in the quality of the film surfaces and negatively affected the structural coloration. The final, successful approach in creating smooth, reproducible calcium alginate films involved using an aerosolized spray of $CaCl_2$ solution. This light mist of solution delivered the Ca^{2+} ions to the films without disturbing their surface structures, an important consideration for maintaining even coloration.

To demonstrate the repeatability of the spin-coating deposition process, 24 films were spun from a single solution using identical deposition parameters. Each film was exposed to aerosolized $CaCl_2$ solution for 10 s before being rinsed and

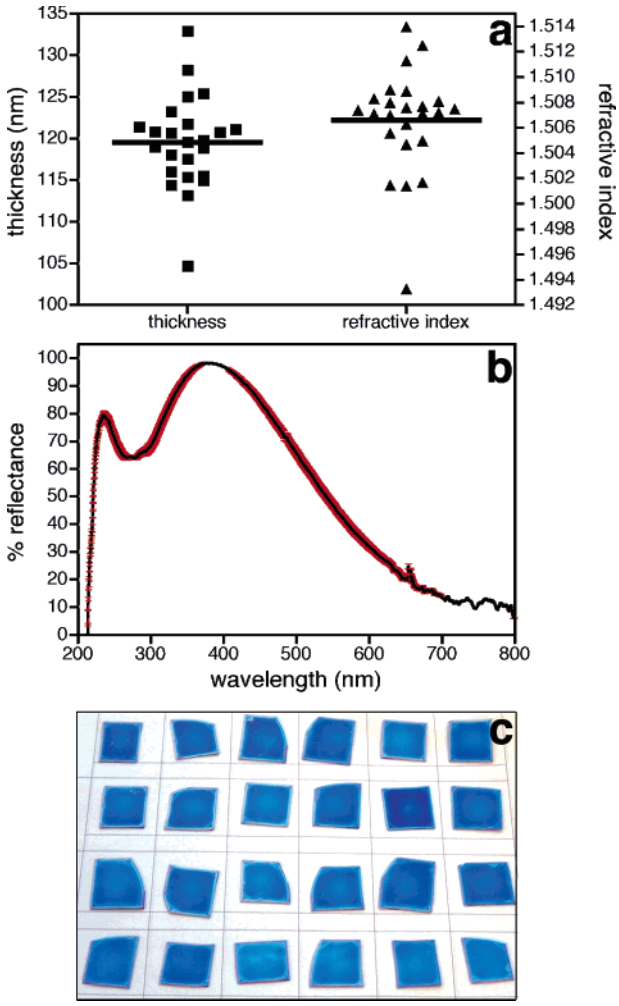

Figure 2. Twenty-four alginate films were made from a single solution using identical spin-coating conditions to demonstrate the repeatability of the deposition process. (a) The films' thicknesses were centered on a value of 119.5 ± 1.1 nm. The Cauchy-calculated refractive index, *n*, at a light wavelength of 589.3 nm was 1.507 ± 0.0008. Lateral spread of data points in each column is used to emphasize clustering of measurements about the mean thickness and refractive index. (b) The reflectance of the 24 films is plotted as an averaged curve (black) with standard error (red). The mean reflectance maximum was measured at 379.3, with little standard error among the samples (±2.9 nm). (c) The films exhibit a brilliant blue color and smooth surface.

dried. This aerosol application technique allows the calcium to be evenly applied over the film's surface without the problems associated with directly dipping the films into solution. The evenness of cross-linking is evidenced by the films' retained smoothness and virtually constant radial coloration from the center to the edge. The thickness, refractive index, and reflectance properties of the films were analyzed and are reported in Figure 2. The 24 samples had an average reflectance maximum of 379.3 nm (±2.9 nm), a thickness of 119.5 nm (±1.1 nm), and a refractive index of 1.507 (±0.0008).

Control over the structural coloration of alginate films is also highly tunable. Films of various thicknesses were produced with a wide variety of reflected colors. Because of the short duration of the Ca^{2+} cross-linking cycle, it is possible to rapidly coat multiple layers of cross-linked alginate on the substrate to achieve different reflectance effects. However, it is also possible to adjust reflectance properties in a single coating by varying the polymer solution viscosity (through the concentration, molecular weight, pH, temperature, etc.) and processing variables (spin-coating velocity, acceleration, and duration). The thin films shown in Figure 3 are all one-layer samples produced in a single application cycle and illustrate the versatile control over film coloration.

The visible regime reflectance profiles accompanying the image in Figure 3 show a comparison between experimental reflectance measured with the fiber optic reflectance spectrometer (solid curves) and model reflectance calculated with thickness and refractive index parameters determined by ellipsometry (dashed curves). The experimental and modeled spectra have been normalized (with the smallest and largest values from each data set scaled to 0% and 100% reflectance, respectively). The modeling software used thickness and index dispersion data to predict, with good accuracy, the wavelength position of minima and maxima along the reflectance curve. Deviations in the normalized reflectance intensity along the vertical axis may be rooted in approximations and assumptions used in the modeling calculations, but may also be an indication of slight color heterogeneity at different points in the films' surfaces. This effect becomes more pronounced as the film thickness increases and the surface topology becomes less planar, producing slight color variations that are visible to the unaided eye (particularly in the magenta and orange films). Because the samples were measured using two different instruments (with similar but slightly different sample spot sizes), it was impossible to ensure that a film was measured at precisely the same spot on both instruments. Nonetheless, the modeled data generated by the ellipsometer were a good match for the reflectance observed experimentally, providing confirmation that the physical and optical parameters measured by the ellipsometer are experimentally sound.

EDTA Treatment. Previous research of alginate microspheres cross-linked with Ca^{2+} ions has indicated that cross-linking is reversible if samples are exposed to a calcium ion chelating agent, such as EDTA.[41] To demonstrate that calcium ions are responsible for the films' water stability, samples that had been cross-linked with $CaCl_2$ solution for 10 s were immersed in neutralized solutions of EDTA at concentrations as low as 0.001 M. Control measurements were made using identical films in ultrapure water. The mean initial film thickness was 117.3 ± 1.4 nm. The samples exposed only to water underwent no statistically significant changes in thickness, varying from the initial measurements by 0.5 ± 0.9 nm. All films treated with EDTA solution were completely dissolved and were no longer detectable by ellipsometry or reflectance. Therefore, we are confident that thin film integrity is maintained by coordination interactions between negatively charged alginate chains and divalent calcium cations in a process that can be reversed by the addition of a calcium chelating agent.

FTIR. The FTIR spectrum of an alginate film subjected to sprayed $CaCl_2$ solution was studied to identify spectral features associated with Ca^{2+} binding. The FTIR spectrum of a Ca-treated alginate film is presented in Figure 4, along with the spectrum of a similarly prepared but non-cross-linked sodium alginate film. Previously published research on bulk samples has indicated a number of key differences in the spectra of sodium and calcium alginate,[27,42,43] and several of these features are observed in the FTIR spectra of the two films. In the Ca^{2+}-cross-linked alginate sample, there is a general broadening of the peaks at ~1630 and 1420 cm^{-1}, representing the asymmetric and symmetric stretches of the COO^- group. The signal near 1420 cm^{-1} in cross-linked alginate is reduced in intensity when compared to the corresponding signal in the non-cross-linked sodium alginate sample and is shifted to higher frequency in the presence of Ca^{2+}, from 1415 to 1420 cm^{-1}.[42] The asym-

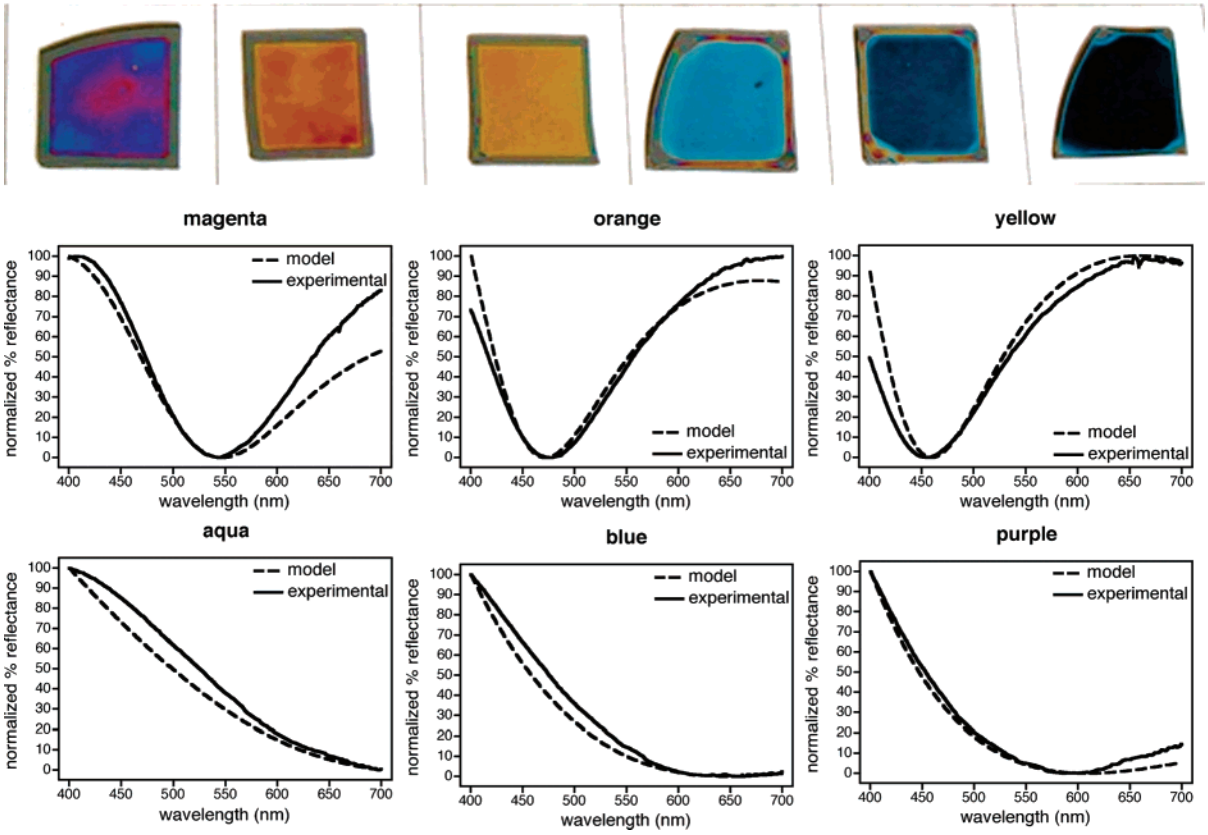

Figure 3. Film thickness can be tuned with solution viscosity and spin-coating velocity. The thicknesses of these films (nm) are 266.5 (magenta), 226.2 (orange), 219.9 (yellow), 122.4 (aqua), 102.8 (blue), and 95.8 (purple). The mean refractive index is 1.521. Normalized reflectance spectra in the visible wavelength regime (solid curves, measured from reflectance spectrometry) are shown for each film, along with the model predictions for the same wavelength range (dashed curves, calculated using ellipsometer-determined thickness and index values). There is good agreement between the positioning of minima and maxima in measured and modeled reflectance curves.

metric stretch is also shifted higher, from 1628 to 1638 cm^{-1}. This upshifting trend of the carboxylate stretches for calcium alginate relative to sodium alginate is in agreement with signal position movement (from 1416.80 to 1424.23 cm^{-1} for C−O and from 1620.17 to 1633.8 cm^{-1} for C═O) reported by Volesky.[19,44]

The region between 1150 and 1000 cm^{-1} features strong signals caused by C−C and C−O stretching. The signal at 1090 cm^{-1} is attributed to C−O stretching and is considerably strengthened in the spectrum of Ca^{2+}-cross-linked alginate. This enhanced peak is likely the result of increased strain of the carboxyl C−O as it stretches to accommodate the coordination structure around the Ca^{2+} ion. The C−C stretch near 1040 cm^{-1} is shifted to lower frequencies (from 1042 to 1038 cm^{-1}) in response to the presence of Ca^{2+}, as previously reported. Also apparent is the emergence of an unidentified peak near 1264 cm^{-1}, which appears in other published spectra of calcium alginate.[42,43]

Ion Study. Alginate films were given a brief exposure to 50 ppm solutions containing a variety of ionic species from dissolved salts. Divalent cationic species tested include Hg, Pb, Cd, Co, and Ni. Trivalent cationic species tested include As and Cr. The anions in these salts were nitrates (Hg, Pb, Cr), chlorides (Cd, Cr), oxides (As), sulfates (Ni), and acetates (Co, Pb). Film responses to nitrate, chloride, sulfate, and acetate counterions were evaluated using sodium salts. Additionally, the film response was measured for hexavalent chromium oxide, existing primarily as the divalent oxyanionic species chromate $(CrO_4)^{2-}$ at neutral pH, and for disodium hydrogen phosphate, existing as $(H_2PO_4)^-$ and $(HPO_4)^{2-}$ at neutral pH.

General trends in the changes of the film thickness, refractive index, and reflectance maximum in response to 50 ppm ionic solutions are summarized in Table 1. Values in bold type were found to be statistically significant in *t* test analyses. The data from the ion study suggest that changes in alginate film reflectance after selective ion exposure are caused by a combination of physical and optical changes within the films.

In some cases, most notably with the Cr solutions, physical changes in film thicknesses make up the predominant response. The Cr(VI) solution caused a negative change in thickness and blue-shifting of the reflectance maximum, while both Cr(III) species caused increases in thickness and red-shifting of the reflectance maximum. In the case of all chromium species, the changes in film reflection were visible to the unaided eye.

The strong change of thickness response of the films to Cr(VI) may seem paradoxical, since the negatively charged polymer backbone might inhibit binding of the negatively charged chromate oxyanions. However, it has been noted that Cr(VI) adsorption onto binary biopolymeric beads of calcium alginate and gelatin linearly increases with alginate content.[45] The gelatin and alginate components impart positive and negative charge to the beads, respectively. The relationship between alginate content and Cr(VI) sorption has been attributed to hydrogen-bonding effects between the $HCrO_4^-$ anions and negatively charged sites along the alginate chain or interaction with the calcium ion cross-linker.

While hexavalent chromium caused the largest negative change in film thickness, exposure of films to trivalent chromium led to the largest measured positive thickness change. This is suggestive that different mechanisms are involved in

Table 1. Thin Film Measurements after Immersion in 50 ppm Ionic Solutions

50 ppm solution	Δ(thickness)[a,b] (nm)	Δn[a,b]	reflectance max shift[a,c] (nm)
chromium(VI) (*oxide*)	**−19.1 ± 1.0**	−0.002 ± 0.007	**−46.6 ± 0.4**
mercury(II) (*nitrate*)	**−7.2 ± 0.6**	**0.020 ± 0.001**	**−13.4 ± 2.9**
lead(II) (*nitrate*)	**−4.8 ± 1.8**	**0.045 ± 0.015**	**−8.3 ± 0.5**
cadmium(II) (*chloride*)	−2.8 ± 1.6	0.025 ± 0.009	**−5.5 ± 0.9**
arsenic(III) (*oxide*)	−1.6 ± 0.7	0.002 ± 0.002	−4.4 ± 2.0
water	−0.8 ± 2.6	−0.001 ± 0.003	0.5 ± 0.5
(*sodium*) nitrate	0.2 ± 1.1	−0.003 ± 0.002	−2.1 ± 0.9
cobalt(II) (*acetate*)	0.5 ± 0.7	0.000 ± 0.007	**−6.0 ± 0.4**
(*disodium hydrogen*) phosphate	0.8 ± 1.6	**−0.007 ± 0.002**	−0.4 ± 0.6
(*sodium*) chloride	0.9 ± 0.6	**−0.006 ± 0.001**	−0.2 ± 0.4
(*sodium*) sulfate	1.4 ± 1.4	−0.005 ± 0.002	−0.2 ± 0.5
lead(II) (*acetate*)	**2.8 ± 0.9**	**0.057 ± 0.002**	**8.5 ± 0.4**
nickel(II) (*sulfate*)	**3.5 ± 1.0**	0.002 ± 0.001	**6.4 ± 0.4**
(*sodium*) acetate	**4.0 ± 0.6**	**−0.005 ± 0.002**	0.4 ± 1.7
chromium(III) (*nitrate*)	**7.2 ± 0.4**	**−0.010 ± 0.007**	**16.0 ± 0.9**
chromium(III) (*chloride*)	**14.7 ± 0.9**	−0.007 ± 0.010	**32.1 ± 0.8**

[a] Values in bold type denote statistically significant changes, as determined by *t* tests. The error is reported as the standard error of the mean from three independent replicate measurements. [b] Thickness and refractive index data measured using the ellipsometer. Mean initial film thickness 119.5 ± 1.1 nm and mean refractive index $n = 1.510 \pm 0.004$. [c] Reflectance data measured using the reflectance spectrometer. Mean reflectance maximum 346.4 ± 1.6 nm.

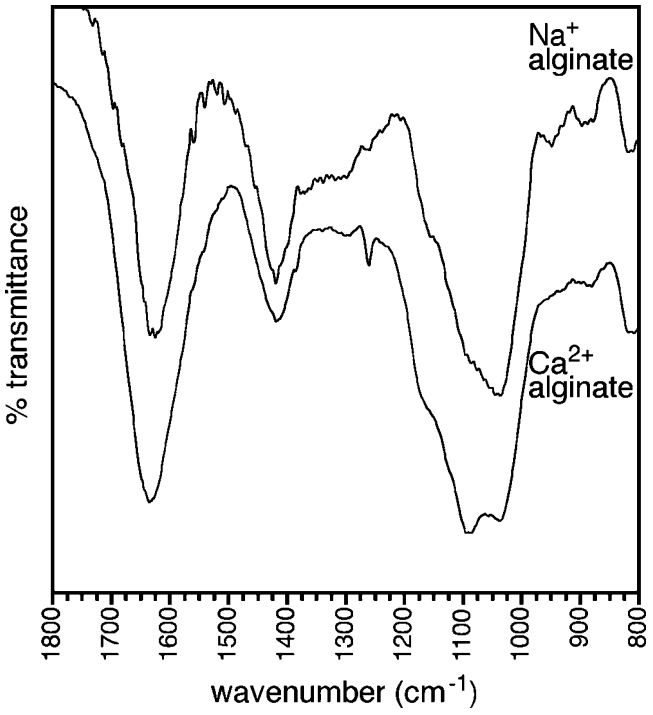

Figure 4. The FTIR spectra of un-cross-linked sodium alginate and cross-linked calcium alginate feature several key signal differences, most especially the enhancement of the C−O stretch near 1090 cm^{-1} in the cross-linked specimen, in response to the formation of the coordination sphere around the Ca^{2+} ion.

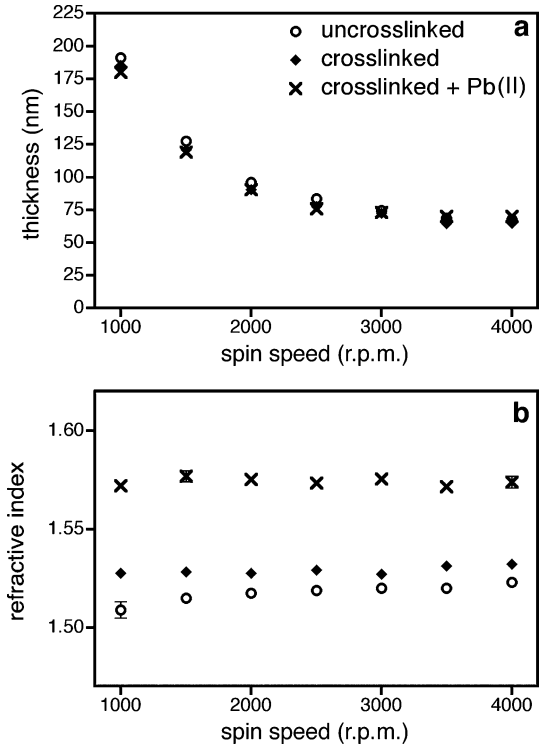

Figure 5. Thickness and refractive index measurements track changes in thin films, coated at different spin speeds, in their initial non-cross-linked states, after cross-linking with Ca^{2+} and finally after exposure to 50 ppm Pb(II) in lead(II) acetate solution. (a) Thickness measurements can be directly correlated to the spinning velocity in the coating process and follow an exponential decay curve as velocity increases. Because of the relatively small thickness change associated with cross-linking and Pb(II) exposure, there is overlap in the data points. (b) Measurements of refractive index remain essentially unperturbed by changes thin film processing speed and are not tied to initial film thicknesses. There is clearly a discernible difference between measurements of films in various states: un-cross-linked (mean $n = 1.518 \pm 0.002$), cross-linked (mean $n = 1.529 \pm 0.001$), and Pb(II)-exposed (mean $n = 1.575 \pm 0.001$).

the interaction between alginate and the two valencies. Work by Ibáñez et al. indicated that the uptake of trivalent Cr in cross-linked alginate beads is mediated by interactions with the carboxylic functional group, as opposed to the coordination process responsible for Ca^{2+} that also involves other oxygen atoms in the alginate subunits.[46,47] The authors concluded that heavy metal cations such as Cr(III) do not displace the coordinated Ca^{2+} (or cross-linking ions). However, the presence of heavy metal species was coupled with a release of protons, suggesting that cations such as Cr^{3+} were being ion exchanged with H^+ from protonated carboxylic groups. This is in agreement with the conclusion by Haug and Smidsroed that binding metals were competing with protons for organic binding spots along

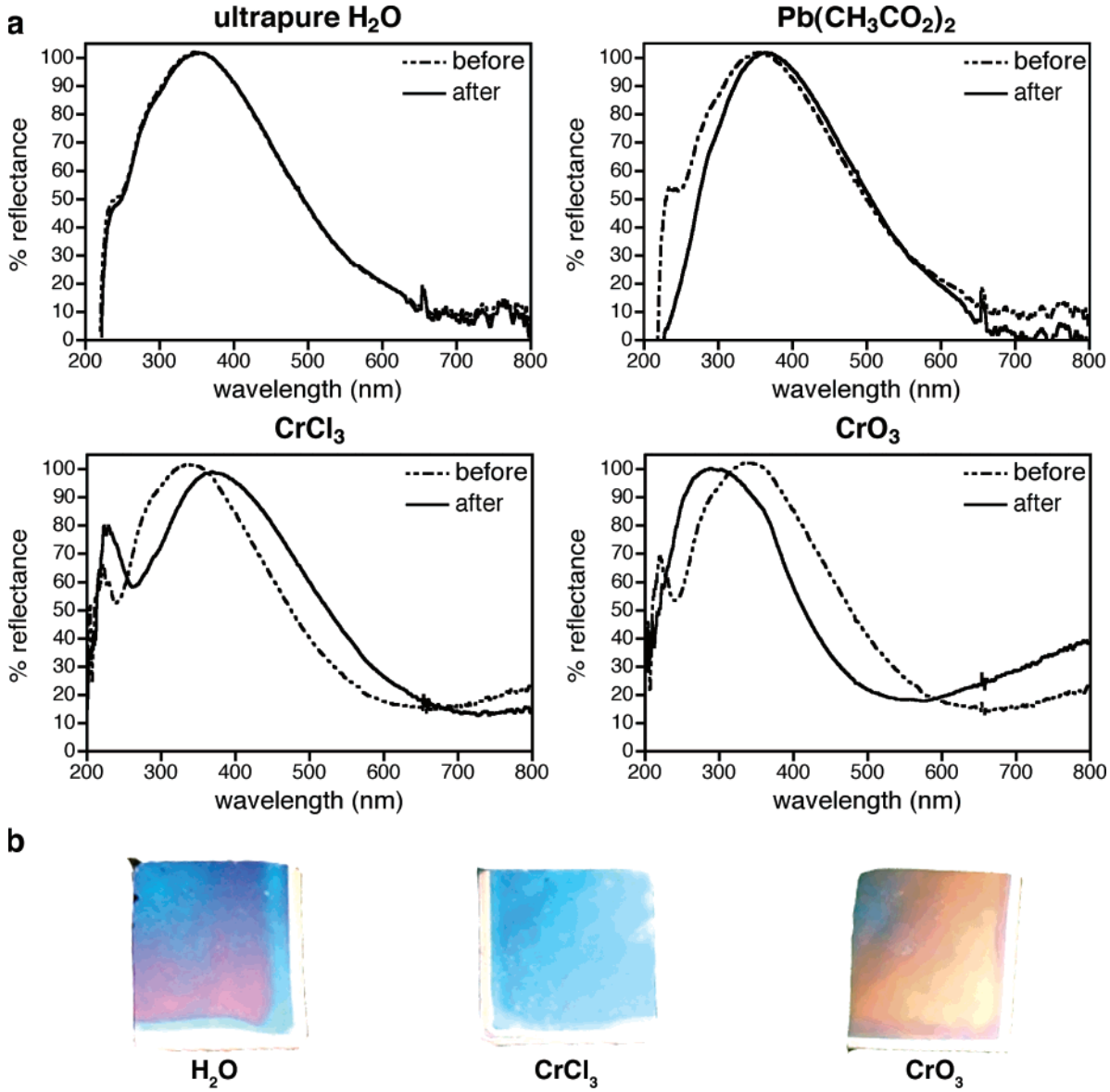

Figure 6. (a) The reflectance profiles of thin films are shown before and after 5 min exposure to water and 50 ppm ionic solutions. Predictably, there is essentially no reflectivity change after exposure to water, since water causes only negligible changes in thickness and refractive index. The reflectance of films exposed to 50 ppm Pb(II) solution (acetate counterion) features a small but discernible change in the reflectance maximum and an overall change in the curve shape. This reflectance shift is attributed to a combination of moderate thickness and significant refractive index changes. The chromium(VI) oxide and chromium(III) chloride solutions cause large film thickness changes, leading to large reflectivity shifts. In both cases, the reflectivity response to chromium is predominantly mediated by large changes in film thickness. (b) Three film samples (small pieces taken from one larger film) are shown after exposure to water and Cr(III) and Cr(VI) solutions. The red- and blue-shifting caused by alginate interactions with the two chromium species is readily apparent.

the alginate chain.[21] As illustrated in Figure 1b, cross-linked alginate does feature free carboxylic (or negatively charged carboxylate) groups not involved in the Ca^{2+} coordination. These groups are free to participate in noncomplexed metal uptake.

We have studied film thickness changes in response to three of the metal ions that were also investigated by Ibáñez and his colleagues. Their findings of metal uptake from solutions of $CoSO_4$, $NiSO_4$, and $Cr(NO_3)_3$ (35, 43 and 75 mg/g of alginate beads, respectively)[46] follow the same increasing trend as the film thickness changes we report for solutions from similar salts (0.5, 3.5, and 7.2 nm positive thickness changes, respectively).

The response of alginate thin films to 50 ppm Pb(II) (from both the nitrate and acetate salts) appears rooted in a moderate change in physical dimension and a relatively large shift in optical properties. The refractive index increase of 0.057 caused by lead(II) acetate is the largest shift of *n* measured among the solutions in this study. This refractive index response to Pb(II) was predictably constant among films of different initial thicknesses, which were produced by spin coating at different speeds (Figure 5). The measured effect of 50 ppm Pb(II) on the physical thickness of alginate films is not extreme, and use of this physical property as a diagnostic for the presence of lead requires that the experimenter have knowledge of the film's dimensions both before and after lead exposure. However, no such information is required if the refractive index can be measured. The ellipsometer is able to clearly differentiate between calcium alginate thin films exposed to Pb(II) ions using only a single refractive index measurement, without information about changes in film thickness or reflectance.

Reflectance profiles of thin films before and after exposure to pure water and 50 ppm solutions of lead(II) acetate, chromium(III) chloride, and chromium(VI) oxide are shown for

comparison in Figure 6a. As expected, there is negligible reflectance change in response to pure water. The reflectance shift after exposure to lead(II) acetate is illustrative of a case where the change in reflectance maximum is relatively small (from 354.5 to 363.3 nm), but the overall shape of the reflectance curve is significantly changed, particularly in the UV range and the visible and IR range above ~600 nm. The color shifting is subtle, but discernible to the unaided eye. The spectra for the two chromium species are examples of significant lateral shifting of reflected color over a broad range of wavelengths, producing marked changes in visible appearance. The film samples shown in Figure 6b came from a single silicon wafer coated with a cross-linked alginate film. This sample was partitioned into several smaller pieces, so that each piece possessed essentially identical initial color reflectivity. The small wafer fragments were exposed to water and Cr(III) and Cr(VI) solutions. The sample exposed to water exhibited no visually discernible color change from its original blue-violet condition, but the samples exposed to Cr(III) and Cr(VI) exhibit dramatic red- and blue-shifting, respectively.

It is possible to draw a correlation between the refractive index data reported in Table 1 and the conclusions about alginate's affinity for various divalent species drawn by Haug and Smidsroed, who examined the viscosity changes in alginate solutions containing these cations.[21] Haug and Smidsroed concluded that different metals have variable affinities for alginate, as well as variability in the required ionic content to induce gelation. They found that the cation concentration needed to achieve gel formation increased in the following order: Pb < Cd < Ni < Co. Our refractive index measurements are in agreement with Haug and Smidsroed's ordering sequence: Pb ($\Delta n = 0.045$ for nitrate salt and 0.057 for acetate salt), Cd ($\Delta n = 0.025$), Ni ($\Delta n = 0.002$), and Co ($\Delta n = 0.000$). We conclude that alginate's high selectivity for Pb(II) allows the lead cation to affect a more substantial change in optical properties, compared with other divalent cations at the same concentration level.

Profilometer Study. Optical profilometry was used to confirm ellipsometer-measured thickness changes of two selected ion solutions, lead(II) acetate and chromium(VI) oxide. The Pb(II) and Cr(VI) species were chosen for this experiment because they caused marked changes in film thickness and refractive index, respectively, in the metal ion studies performed on the ellipsometer.

The profilometer registered a thickness increase of 2.8 ± 2.6 nm in the films exposed to the Pb(II) solution, in excellent agreement with measurements performed using the ellipsometer of 2.8 ± 0.9 nm. The samples exposed to Cr(VI) registered a decrease in thickness of -25.3 ± 0.5 nm, similar to the ellipsometer measured change of -19.1 ± 1.0 nm. These profilometry measurements are further evidence that significantly different changes of thickness occurred in response to the two solutions, with good correlation between ellipsometer and profilometer measurements (within profilometer accuracy for thin films of this size scale). The films' optical responses to Pb(II) and Cr(VI) represent two extremes in the optical film response: one in which the cause of reflectance shift is dominated by a change in effective refractive index and another in which the reflectance shift is primarily caused by a change in film thickness.

Conclusions

Solutions of the biopolymer alginate have been processed into Ca^{2+}-cross-linked thin films. These films possess structural color, caused by thin film interference of reflected light. Films have been produced with repeatable reflectance properties, as well as with highly tunable reflectivity in a wide array of colors. Once cross-linked with Ca^{2+}, the alginate films demonstrate excellent water stability. Samples exposed to the cross-linking solution for the minimal time of 10 s underwent no statistically significant change in thickness after 30 min of submersion in water. This water stability of cross-linked alginate is highly desirable for analyte sensing in aqueous solutions, since film response to a targeted analyte must always be normalized against any thickness changes caused by exposure to water (i.e., thickness decreases caused by slight film dissolution or increases caused by water uptake).

These cross-linked alginate thin films were exposed to a variety of metal ion solutions, and corresponding changes in film thickness and/or refractive index were measured. The physical and optical changes led, in many cases, to significant shifts in the reflected structural color. Particularly notable are the large positive and negative changes in thickness associated with differently charged chromium species and the significant shifts in refractive index in response to divalent lead. Ionic species of several other metals, including mercury and nickel, also caused statistically significant changes in reflectance maxima of the films through a combination of thickness and refractive index effects.

Although the results presented here suggest the potential of alginate thin films as a color-based metal sensor, there are a great many challenges to overcome before these films could be used as a comprehensive optical sensing platform for detection of metal ions in complex wastewaters. For instance, in a study of the metal uptake by algal biomass from a solution containing both Cd and Fe ions, it was determined that the uptake of the two metal species was strongly coupled.[48] This sort of susceptibility to interference by other codissolved metal species, as well as countless other potentially interfering biological and organic compounds, would be particularly confounding in a complex sample from a source such as a public water supply or a river system. It would also be necessary to consider a number of complicating factors such as pH, ionic strength, and temperature and their effect on the uptake of metals by the films and corresponding reflectance changes. However, further research in increasing alginate's selectivity and sensitivity (through the use of alginates with different M/G ratios, different cross-linking strategies, and chemical modifications) might make optical-based detection of real-world samples more feasible using a multiplex dipstick of different thin films, each with a different sensitivity and selectivity for analyte species.

Acknowledgment. M.D.C. thanks the Koerner Family Fellowship, U.S. Department of Education (GAANN), and Drexel University's College of Engineering for support of his graduate studies. C.L.S. thanks the Pennsylvania Department of Health for funding this project. We are grateful to Mr. Greg Pribil of the J.A. Woollam Co. for helpful discussions on ellipsometry and to Dr. Adam Fontecchio of Drexel University for use of the optical profilometer.

Supporting Information Available. Reflectance profiles of Ca^{2+}-cross-linked alginate thin films before and after exposure to 50 ppm ion solutions. This material is available free of charge via the Internet at http://pubs.acs.org.

References and Notes

(1) Vukusic, P.; Shambles, J. R. Photonic structures in biology. *Nature* **2003**, *424*, 852−55.

(2) Crookes, W. J.; Ding, L.-L.; Huang, Q. L.; Kimbell, J. R.; Horwitz, J.; McFall-Ngai, M. J. Reflectins: The unusual proteins of squid reflective tissues. *Science* **2004**, *303* (5655), 235−238.
(3) Parker, A. R. Natural photonic engineers. *Mater. Today* **2002**, *5* (9), 26−31.
(4) Parker, A. R.; Martini, N. Structural colour in animals−simple to complex optics. *Opt. Laser Technol.* **2006**, *38* (4−6), 315−322.
(5) Mathger, L. M.; Land, M. F.; Siebeck, U. E.; Marshall, N. J. Rapid colour changes in multilayer reflecting stripes in the paradise whiptail, Pentapodus paradiseus. *J. Exp. Biol.* **2003**, *206* (20), 3607−3613.
(6) Parker, A. R.; McPhedran, R. C.; McKenzie, D. R.; Botten, L. C.; Nicorovici, N. A. P. Photonic engineering−Aphrodite's iridescence. *Nature* **2001**, *409* (6816), 36−37.
(7) Kinoshita, S.; Yoshioka, S. Structural colors in nature: The role of regularity and irregularity in the structure. *ChemPhysChem* **2005**, *6* (8), 1442−1459.
(8) Schauer, C. L.; Chen, M. S.; Chatterley, M.; Eisemann, K.; Welsh, E. R.; Price, R. R.; Schoen, P. E.; Ligler, F. S. Color changes in chitosan and poly(allyl amine) films upon metal binding. *Thin Solid Films* **2003**, *434* (1−2), 250−257.
(9) Schauer, C. L.; Chen, M. S.; Price, R. R.; Schoen, P. E.; Ligler, F. S. Colored thin films for specific metal ion detection. *Environ. Sci. Technol.* **2004**, *38* (16), 4409−4413.
(10) Haug, A.; Larsen, B.; Smidsroed, O. Uronic acid sequence in alginate from different sources. *Carbohydr. Res.* **1974**, *32* (*2*), 217−225.
(11) Lamelas, C.; Avaltroni, F.; Benedetti, M.; Wilkinson, K. J.; Slaveykova, V. I. Quantifying Pb and Cd complexation by alginates and the role of metal binding on macromolecular aggregation. *Biomacromolecules* **2005**, *6* (5), 2756−2764.
(12) Davis, T. A.; Volesky, B.; Mucci, A. A review of the biochemistry of heavy metal biosorption by brown algae. *Water Res.* **2003**, *37* (18), 4311−4330.
(13) Kuyucak, N.; Volesky, B., The Mechanism of Cobalt Biosorption. *Biotechnol. Bioeng.* **1989**, *33* (*7*), 823−831.
(14) Raize, O.; Argaman, Y.; Yannai, S. Mechanisms of biosorption of different heavy metals by brown marine macroalgae. *Biotechnol. Bioeng.* **2004**, *87* (*4*), 451−458.
(15) Figueira, M. M.; Volesky, B.; Ciminelli, V. S. T.; Roddick, F. A. Biosorption of metals in brown seaweed biomass. *Water Res.* **2000**, *34* (*1*), 196−204.
(16) Draget, K. I.; Smidsroed, O.; Skjak-Braek, G. Alginates from algae. In *Polysaccharides and polyamides in the food industry: properties, production, and patents*; Steinbuchel, A., Rhee, S. K., Eds.; John Wiley & Sons: Weinheim, Germany, 2005; Vol. 1.
(17) Davis, T. A.; Llanes, F.; Volesky, B.; Mucci, A. Metal selectivity of Sargassum spp. and their alginates in relation to their alpha-L-guluronic acid content and conformation. *Environ. Sci. Technol.* **2003**, *37* (2), 261−267.
(18) Crist, R. H.; Martin, J. R.; Guptill, P. W.; Eslinger, J. M.; Crist, D. R. Interaction of Metals and Protons with Algae. 2. Ion-Exchange in Adsorption and Metal Displacement by Protons. *Environ. Sci. Technol.* **1990**, *24* (3), 337−342.
(19) Fourest, E.; Volesky, B. Contribution of sulfonate groups and alginate to heavy metal biosorption by the dry biomass of Sargassum fluitans. *Environ. Sci. Technol.* **1996**, *30* (1), 277−282.
(20) Haug, A.; Smidsroed, O. Selectivity of some anionic polymers for divalent metal ions. *Acta Chem. Scand.* **1970**, *23* (3), 843−54.
(21) Haug, A.; Smidsroed, O. The effect of divalent metals on the properties of alginate solutions. II. Comparison of different metal ions. *Acta Chem. Scand.* **1965**, *19* (2), 341−51.
(22) Smidsroed, O.; Haug, A. The effect of divalent metals on the properties of alginate solutions. I. Calcium ions. *Acta Chem. Scand.* **1965**, *19* (2), 329−40.
(23) Schweiger, R. G. Acetylation of alginic acid. II. Reaction of algin acetates with calcium and other divalent ions. *J. Org. Chem.* **1961**, *27* (5), 1789−91.
(24) Yokoyama, F.; Achife, C. E.; Takahira, K.; Yamashita, Y.; Monobe, K.; Kusano, F.; Nishi, K. Morphologies of oriented alginate gels crosslinked with various divalent metal ions. *J. Macromol. Sci. Phys.* **1992**, *B31* (4), 463−83.
(25) Wang, L.; Shelton, R. M.; Cooper, P. R.; Lawson, M.; Triffitt, J. T.; Barralet, J. E. Evaluation of sodium alginate for bone marrow cell tissue engineering. *Biomaterials* **2003**, *24* (20), 3475−3481.
(26) Becker, T. A.; Kipke, D. R.; Brandon, T. Calcium alginate gel: A biocompatible and mechanically stable polymer for endovascular embolization. *J. Biomed. Mater. Res.* **2001**, *54* (1), 76−86.
(27) Wong, T. W.; Chan, L. W.; Bin Kho, S.; Heng, P. W. S. Design of controlled-release solid dosage forms of alginate and chitosan using microwave. *J. Controlled Release* **2002**, *84* (3), 99−114.
(28) Kuo, C. K.; Ma, P. X. Ionically crosslinked alginate hydrogels as scaffolds for tissue engineering: Part 1. Structure, gelation rate and mechanical properties. *Biomaterials* **2001**, *22* (6), 511−521.
(29) Haug, A. Affinity of some bivalent metals for different types of alginates. *Acta Chem. Scand.* **1961**, *15*, 1794−5.
(30) Schweiger, R. G. Acetylation of alginic acid. I. Preparation and viscosities of algin acetates. *J. Org. Chem.* **1961**, *27* (5), 1786−89.
(31) Grant, G. T.; Morris, E. R.; Rees, D. A.; Smith, P. J. C.; Thom, D. Biological interactions between polysaccharides and divalent cations: The egg-box model. *FEBS Lett.* **1973**, *32* (1), 195−198.
(32) Rees, D. A. Polysaccharide shapes and their interactions−some recent advances. *Pure Appl. Chem.* **1971,** *53*, 1−14.
(33) Mackie, W.; Perez, S.; Rizzo, R.; Taravel, F.; Vignon, M. Aspects of the Conformation of Polyguluronate in the Solid-State and in Solution. *Int. J. Biol. Macromol.* **1983**, *5* (6), 329−341.
(34) Steginsky, C. A.; Beale, J. M.; Floss, H. G.; Mayer, R. M. Structural Determination of Alginic Acid and the Effects of Calcium-Binding as Determined by High-Field NMR. *Carbohydr. Res.* **1992**, *225* (1), 11−26.
(35) Haug, A.; Smidsroed, O. Strontium, Calcium and Magnesium in Brown Algae. *Nature* **1967**, *215* (5106), 1167−1168.
(36) Cass, T.; Ligler, F. S. *Immobilized Biomolecules in Analysis*; Oxford University Press: Oxford, 1999.
(37) Guo, S.; Gustafsson, G.; Hagel, O. J.; Arwin, H. Determination of refractive index and thickness of thick transparent films by variable-angle spectroscopic ellipsometry: application to benzocyclobutene films. *Appl. Opt.* **1996**, *35* (10), 1693−1699.
(38) Elizalde, E.; Frigerio, J. M.; Rivory, J. Determination of thickness and optical constants of thin films from photometric and ellipsometric measurements. *Appl. Opt.* **1986**, *25* (24), 4557−61.
(39) Flock, K. The simultaneous determination of n, k, and t from polarimetric data. *Thin Solid Films* **2004**, *455−456*, 349−355.
(40) Herman, I. P. *Optical Diagnostics for Thin Film Processing*, 1st ed.; Academic Press: San Diego, 1996.
(41) Zhu, H. G.; Srivastava, R.; McShane, M. J. Spontaneous loading of positively charged macromolecules into alginate-templated polyelectrolyte multilayer microcapsules. *Biomacromolecules* **2005**, *6* (4), 2221−2228.
(42) Sartori, C.; Finch, D. S.; Ralph, B.; Gilding, K. Determination of the cation content of alginate thin films by FTIR spectroscopy. *Polymer* **1997**, *38* (1), 43−51.
(43) Sankalia, M. G.; Mashru, R. C.; Sankalia, J. M.; Sutariya, V. B. Papain entrapment in alginate beads for stability improvement and site-specific delivery: Physicochemical characterization and factorial optimization using neural network modeling. *AAPS PharmSciTech* **2005**, *6* (2).
(44) Figueira, M. M.; Volesky, B.; Mathieu, H. J. Instrumental analysis study of iron species biosorption by Sargassum biomass. *Environ. Sci. Technol.* **1999**, *33* (11), 1840−46.
(45) Bajpai, J.; Shrivastava, R.; Bajpai, A. K. Dynamic and equilibrium studies on adsorption of Cr(VI) ions onto binary bio-polymeric beads of cross linked alginate and gelatin. *Colloids Surf., A* **2004**, *236* (1−3), 81−90.
(46) Ibanez, J. P.; Umetsu, Y. Potential of protonated alginate beads for heavy metals uptake. *Hydrometallurgy* **2002**, *64* (2), 89−99.
(47) Ibanez, J. P.; Umetsu, Y. Uptake of trivalent chromium from aqueous solutions using protonated dry alginate beads. *Hydrometallurgy* **2004**, *72* (3−4), 327−334.
(48) Figueira, M. M.; Volesky, B.; Ciminelli, V. S. T. Assessment of interference in biosorption of a heavy metal. *Biotechnol. Bioeng.* **1997**, *54* (4), 344−350.

BM060433F